DALTON
FULL PAPER

Formation and structural relationship of electroactive Pt^{II}–Hg^{II} polymetallic sulfide aggregates

Zhaohui Li, Xingling Xu, Soo Beng Khoo, K. F. Mok * and T. S. Andy Hor *

Department of Chemistry, National University of Singapore, 3 Science Drive 3, Singapore 117543

Received 12th May 2000, Accepted 11th July 2000
Published on the Web 14th August 2000

A series of $\{Pt_2HgS_2\}$, $\{Pt_2Hg_2S_2\}$ and $\{Pt_4HgS_4\}$ complexes, *viz.* $[(Ph_3P)_4Pt_2(\mu_3\text{-}S)_2HgCl_2]$ **2**, $[(Ph_3P)_4Pt_2(\mu_3\text{-}S)_2Hg(PPh_3)]X_2$ [X = Cl (**3a**) or PF_6 (**3b**)], $[HgPt_4(PPh_3)_8(\mu_3\text{-}S)_4]X_2$ [X = PF_6, (**4a**) or ClO_4 (**4b**)], $[Pt_2(Ph_3P)_4(\mu_3\text{-}S)_2Hg_2(\mu\text{-}Cl)_2Cl_2]$ **5**, $[(Ph_3P)_4Pt_2(\mu_3\text{-}S)_2Hg_2(\mu\text{-}Cl)_2(PPh_3)_2][PF_6]_2$ **6** and $[(Ph_3P)_4Pt_2(\mu_3\text{-}S)_2Hg_2(NO_3)_2]X_2$ [X = NO_3 (**7a**) or PF_6 (**7b**)] have been synthesized from $[Pt_2(\mu\text{-}S)_2(PPh_3)_4]$ **1** with the appropriate mercury(II) compounds through 1 : 1, 1 : 2 and 2 : 1 Lewis acid–base additions. Formation of the major product is governed largely by the stoichiometric quantity of the substrates. Reaction intermediates can be isolated and characterized. Their conversions into the final products have been verified. Single-crystal X-ray crystallography on **2**, **3b**, **4b**, **5** and **6** revealed a range of Pt^{II}/Hg^{II} metal sulfide cores with different nuclearities. V.T. $^{31}P\text{-}\{^1H\}$ NMR study of **3b** showed a rapid migration of the $[Hg(PPh_3)]$ moiety between two sulfide sites in a $\{Pt_2HgS_2\}$ core. Cyclic voltammetry was carried out on **2**, **3b**, **5** and **6**. Complex **3b** undergoes an approximately reversible one electron transfer oxidation with $E_{p,a}$ = 1.10 V and $E_{p,c}$ = 1.01 V.

Introduction

The function of $[Pt_2S_2(PPh_3)_4]$, **1**, as a metalloligand in hetero- and inter-metallic syntheses has been well established.[1] However, most of the reported systems are 1 : 1 addition products, *viz*. $\{Pt_2M\}$ systems, with M = Ag/Au^I providing notable exceptions.[2,3] In our desire to build aggregates and clusters that have a higher degree of nanomaterials properties, it is important to extend the current synthetic strategy to the higher nuclearity systems such as $\{Pt_2M_2\}$ and $\{Pt_4M\}$. For such systems to be realized, we believe that two important criteria of the metal (M) must be met: (1) it must show a flexible array of geometries in order to accommodate the ligand and structural changes, and (2) it must have a good affinity for sulfur. Amongst our work on numerous metals, we found that Hg^{II} fulfils these criteria and indeed is able to support a range of high nuclearity networks. In this paper we shall report the synthesis of a series of $\{Pt_2HgS_2\}$, $\{Pt_2Hg_2S_2\}$ and $\{Pt_4HgS_4\}$ systems through 1 : 1, 1 : 2 and 2 : 1 additions, their interconversions, structural relationship and electrochemical behavior. The last property is related to our general interest in electroactive multimetallic materials as electronic nano-devices.

Experimental

All solvents were distilled and deoxygenated by argon before use. Complex **1** was synthesized from $[PtCl_2(PPh_3)_2]$ and $Na_2S{\cdot}2H_2O$ according to the literature method.[4] Other chemicals were used as supplied. Elemental analyses were carried out in the Elemental Analysis Laboratory in the Department of Chemistry, National University of Singapore (NUS). Infrared spectra were taken on KBr discs with a Perkin-Elmer 1600 FT-IR spectrophotometer, $^{31}P\text{-}\{^1H\}$ NMR spectra on a Bruker ACF 300 spectrometer. Conductivity was determined using a STEM conductivity 1000 meter. Cyclic voltammetric measurements were performed with a Model PS-605 Potentiostat (Elchema, New York, USA) together with a Model FG-206F Waveform Generator. Voltammograms were recorded with a WX-1100 x-y recorder (Graphtec Corp., Tokyo, Japan). All experiments were performed in AR grade CH_2Cl_2 that was distilled over P_2O_5 before use. $[Bu_4N][ClO_4]$ (AR grade, dried for 3 days in a vacuum oven) was used as supporting electrolyte (typically 0.1 M). The concentration of the sample was 1.00×10^{-3} M. The reference electrode was $Ag\text{–}Ag^+$ (0.01 M $AgNO_3$, 0.1 M $[Bu_4N][ClO_4]$ in CH_3CN). The working electrode was a glassy carbon disc electrode (diameter 3 mm). All experiments were carried out at ambient temperature (25 ± 2 °C).

Syntheses

$[(Ph_3P)_4Pt_2(\mu_3\text{-}S)_2HgCl_2]{\cdot}CH_2Cl_2$ 2. A mixture of complex **1** (0.150 g, 0.1 mmol) and $HgCl_2$ (0.027 g, 0.1 mmol) was stirred in MeOH (20 cm^3) for 6 h to give a bright yellow suspension. The precipitate was collected by filtration and purified by recrystallization from CH_2Cl_2–hexane to yield yellow crystals of **2** (0.105 g, 54%). Calc. for $C_{73}H_{62}Cl_4HgP_4Pt_2S_2$: C, 47.3; H, 3.3; Cl, 7.7; P, 6.7; S, 3.5%. Found: C, 46.7; H, 3.4; Cl, 7.9; P, 6.9; S, 3.7%. Λ_m (10^{-3} mol dm^{-3}, CH_2Cl_2) 3.2 Ω^{-1} cm^2 mol^{-1}. $^{31}P\text{-}\{^1H\}$ NMR (CD_2Cl_2): δ 19.7 (4P, ^1J(P–Pt) 3016 Hz).

$[(Ph_3P)_4Pt_2(\mu_3\text{-}S)_2Hg(PPh_3)]X_2{\cdot}H_2O$ (X = Cl (3a) or PF_6 (3b)). A mixture of complex **1** (0.150 g, 0.1 mmol) and $[HgCl_2(PPh_3)_2]$ (0.079 g, 0.1 mmol) was stirred in MeOH (20 cm^3) for 1 h to give a bright yellow solution. Addition of Et_2O led to the isolation of a yellow precipitate of **3a**. Metathesis with NH_4PF_6 yielded **3b**, which was purified by recrystallization from CH_2Cl_2–MeOH to give yellow crystals (0.099 g, 45%). Calc. for $C_{90}H_{77}F_{12}HgOP_7Pt_2S_2$: C, 47.5; H, 3.4; F, 10.0; P, 9.5; S, 2.8%. Found: C, 46.4; H, 3.3; F, 10.4; P, 9.3; S, 3.0%. IR (cm^{-1}): 839vs (PF_6^-). Λ_m (10^{-3} mol dm^{-3}, Acetone) 158.3 Ω^{-1} cm^2 mol^{-1}. $^{31}P\text{-}\{^1H\}$ NMR (CD_2Cl_2): δ 16.2 (4P, ^1J(P–Pt) 3160) and 34.8 ppm (1P, ^1J(P–Hg) 4872 Hz).

Complex **3b** can also be prepared by stirring a mixture of **2** (0.095 g, 0.05 mmol) and PPh_3 (0.013 g, 0.05 mmol) in MeOH followed by a metathesis reaction with NH_4PF_6. Yield: 0.054 g, 49%.

DOI: 10.1039/b003799k

$[HgPt_4(PPh_3)_8(\mu_3\text{-}S)_4]X_2$ (X = PF_6 (4a) or ClO_4, (4b)). *From complex* ***1*** *and* $[HgCl_2(PPh_3)_2]$. A mixture of complex **1** (0.150 g, 0.1 mmol) and $[HgCl_2(PPh_3)_2]$ (0.040 g, 0.05 mmol) was stirred in MeOH (40 cm^3) overnight. Addition of Et_2O to the resultant golden yellow solution gave a yellow precipitate, which was isolated and purified by metathesis with NH_4PF_6 in MeOH. Recrystallization from CH_2Cl_2–MeOH gave yellow crystals of **4a** (0.064 g, 37%). Calc. for $C_{144}H_{120}F_{12}HgP_{10}Pt_4S_4$: C, 49.4; H, 3.4; P, 8.9; S, 3.7%. Found: C, 48.8; H, 3.5; P, 8.5; S, 3.8%. IR (cm^{-1}): 839vs (PF_6^-). ^{31}P-{^1H} NMR (CD_2Cl_2): δ 18.1 (4P, ^1J(P–Pt) 3290) and 14.3 (4P, ^1J(P–Pt) 2960 Hz).

From complex ***1*** *and* ***2*** *or* ***3***. Complex **4a** can also be prepared by stirring a mixture of **2** (0.059 g, 0.033 mmol) and **1** (0.05 g, 0.033 mmol) in MeOH followed by a metathesis reaction with NH_4PF_6. Yield: 0.065 g, 56%. It can be prepared similarly by mixing **3a** (0.081 g, 0.04 mmol) and **1** (0.061 g, 0.04 mmol) in MeOH followed by a metathesis reaction with NH_4PF_6. Yield: 0.073 g, 52%.

From complex ***1*** *and* $Hg(ClO_4)_2$. A mixture of complex **1** (0.150 g, 0.1 mmol) and $Hg(ClO_4)_2 \cdot 7H_2O$ (0.037 g, 0.05 mmol) was stirred in MeOH (40 cm^3) for 2 h. The suspension, changing gradually from orange to yellow, was filtered and the mother liquor treated with Et_2O to yield a yellow precipitate, which was purified by recrystallization from CH_2Cl_2–hexane to yield yellow crystalline **4b** (0.044 g, 23%). Calc. for $C_{144}H_{120}Cl_2HgO_8P_8Pt_4S_4$: C, 50.7; H, 3.5; Cl, 2.1; P, 7.3; S, 3.8%. Found: C, 51.3; H, 3.5; Cl, 2.3; P, 7.0; S, 3.6%. Λ_m (10^{-3} mol dm^{-3}, CH_2Cl_2) 126.5 Ω^{-1} cm^2 mol^{-1}. ^{31}P-{^1H} NMR (CD_2Cl_2): δ 18.5 (4P, ^1J(P–Pt) 3290) and 14.4 (4P, ^1J(P–Pt) 2960 Hz).

$[(Ph_3P)_4Pt_2(\mu_3\text{-}S)_2Hg_2(\mu\text{-}Cl)_2Cl_2]\cdot CH_2Cl_2$ 5. A mixture of complex **1** (0.15 g, 0.1 mmol) and $HgCl_2$ (0.054 g, 0.2 mmol) was stirred in MeOH for 4 h. The suspension changed gradually from orange to pale yellow. The precipitate was collected by filtration and purified by recrystallization from CH_2Cl_2–MeOH to yield **5** as pale yellow crystals (0.087 g, 43%). Calc. for $C_{73}H_{62}Cl_6Hg_2P_4Pt_2S_2$: C, 41.3; H, 2.9; Cl, 10.0; P, 5.8; S, 3.0%. Found: C, 41.7; H, 3.0; Cl, 8.7; P, 6.0; S, 3.2%. Λ_m (10^{-3} mol dm^{-3}, CH_2Cl_2) 4.8 Ω^{-1} cm^2 mol^{-1}. ^{31}P-{^1H} NMR (CD_2Cl_2): δ 21.6 (4P, ^1J(P–Pt) 2999 Hz).

$[(Ph_3P)_4Pt_2(\mu_3\text{-}S)_2Hg_2(\mu\text{-}Cl)_2(PPh_3)_2][PF_6]_2\cdot CH_2Cl_2$ 6. A mixture of complex **5** (0.092 g, 0.045 mmol) and PPh_3 (0.024 g, 0.092 mmol) was stirred in MeOH. The pale suspension changed to a clear pale yellow solution within 1 h. This was treated with NH_4PF_6 to yield a precipitate, which was collected and purified by recrystallization from CH_2Cl_2–MeOH to give pale yellow crystals of **6** (0.064 g, 50%). Calc. for $C_{109}H_{92}Cl_4F_{12}Hg_2P_8Pt_2S_2$: C, 45.5; H, 3.2; Cl, 4.9; P, 8.6; S, 2.2%. Found: C, 45.8; H, 3.2; Cl, 3.9; P, 8.7; S, 2.3%. Λ_m (10^{-3} mol dm^{-3}, Acetone) 160.5 Ω^{-1} cm^2 mol^{-1}. ^{31}P-{^1H} NMR (CD_2Cl_2): δ 19.9 (4P, ^1J(P–Pt) 3066) and 34.9 (2P, ^1J(P–Hg) 5490 Hz).

Complex **6** can also be prepared from **1** (0.075 g, 0.05 mmol) and $[HgCl_2(PPh_3)_2]$ (0.080 g, 0.1 mmol) followed by a metathesis reaction with NH_4PF_6. Yield: 0.075 g, 54%.

$[(Ph_3P)_4Pt_2(\mu_3\text{-}S)_2Hg_2(NO_3)_2]X_2$ (X = NO_3 (7a) or PF_6 (7b)). A mixture of complex **1** (0.15 g, 0.1 mmol) and $Hg(NO_3)_2 \cdot 2H_2O$ (0.062 g, 0.2 mmol) was stirred in MeOH for 4 h. The suspension changed gradually from orange to pale yellow. The precipitate was filtered off and addition of Et_2O led to the isolation of a yellow precipitate of **7a**. This was treated with NH_4PF_6 to give a yellow precipitate which was recrystallized from CH_2Cl_2–hexane to yield **7b** as yellow crystals (0.075 g, 35%). Calc. for $C_{36}H_{30}F_6HgNO_3P_3PtS$: C, 37.4; H, 2.6; N, 1.2; P, 8.0; S, 2.8%. Found: C, 37.9; H, 2.4; N, 1.3; P, 7.7; S, 2.5%. Λ_m (10^{-3} mol dm^{-3}, CH_2Cl_2) 128 Ω^{-1} cm^2 mol^{-1}. ^{31}P-{^1H} NMR (CD_2Cl_2): δ 18.7 (4P, ^1J(P–Pt) 3033 Hz).

Crystallography

Single crystals of complexes **2** and **4b** suitable for X-ray diffraction studies were obtained from CH_2Cl_2–hexane by slow diffusion while those of **3b, 5** and **6** were grown from CH_2Cl_2–MeOH (1 : 3) by slow evaporation at r.t. in air. The crystals were unstable due to the loss of the solvates upon isolation and were hence sealed in a quartz capillary with the mother liquor during data collection. Data collections of all five crystals were carried out on a Siemens CCD SMART system. Details of crystal and data collection parameters are summarized in Table 1.

The structures of the five complexes were solved by direct methods and Fourier difference maps. Full-matrix least-squares refinements were carried out with anisotropic thermal parameters for all non-hydrogen atoms except for fluorine atoms which were refined isotropically. Hydrogen atoms were placed on calculated positions (C–H 0.96 Å) and assigned isotropic thermal parameters riding on their parent atoms. Initial calculations were carried out on a PC using SHELXTL PC software package; SHELXL 93 was used for the final refinements.[5] Corrections for absorption were carried out by the SADABS method.[19] The *R* factor of complex **5** is undesirably high because the crystal deteriorated during data collection. There are otherwise no complications in the structure solution.

CCDC reference number 186/2085.

See http://www.rsc.org/suppdata/dt/b0/b003799k/ for crystallographic files in .cif format.

Results and discussion

Syntheses

The preparations of complexes **2–7** and their interconversions are summarized in Scheme 1. Equimolar addition of $HgCl_2$ to **1** in MeOH readily gives $[(Ph_3P)_4Pt_2(\mu_3\text{-}S)_2HgCl_2]$ **2**, which reacts with an excess of PPh_3 to give $[(Ph_3P)_4Pt_2(\mu_3\text{-}S)_2Hg(PPh_3)]Cl_2$ **3a**. Metathesis of **3a** with NH_4PF_6 gives $[(Ph_3P)_4Pt_2(\mu_3\text{-}S)_2Hg(PPh_3)][PF_6]_2$ **3b**. **2** and **3a** can easily be converted into $[HgPt_4(PPh_3)_8(\mu_3\text{-}S)_4][PF_6]_2$ **4a** in the presence of an equimolar quantity of **1** followed by metathesis with NH_4PF_6. The stability gained by the chelating effect of a dithio-like ligand probably provides the driving force of these ligand replacement reactions. Complexes **4a** and **4b** can also be prepared in a one-pot reaction directly from **1** with $HgCl_2$, $[HgCl_2(PPh_3)_2]$ or $Hg(ClO_4)_2$ in 2 : 1 molar ratio. Complex **2** takes up a mole equivalent of $HgCl_2$ to give $[(Ph_3P)_4Pt_2(\mu_3\text{-}S)_2Hg_2(\mu\text{-}Cl)_2Cl_2]$ **5**, which can also be prepared directly from **1** and $HgCl_2$ in 1 : 2 ratio. The two terminal chlorides in **5** can easily be substituted by PPh_3 to give $[(Ph_3P)_4Pt_2(\mu_3\text{-}S)_2Hg_2(\mu\text{-}Cl)_2(PPh_3)_2][PF_6]_2$ **6**. Similarly, **6** can also be prepared directly from **1** and $[HgCl_2(PPh_3)_2]$ in a 1 : 2 ratio or from **3** and $[HgCl_2(PPh_3)_2]$ in a 1 : 1 ratio. Addition of $Hg(NO_3)_2$ to **1** (1 : 2) gives **7**. These syntheses indicate that larger aggregates can be assembled in sequence, stepwise or in one-pot manners. It also suggests that the present system is suitable for the assembly of larger aggregates through a careful choice of metal addition and/or ligand displacement reactions. Intermediates can be isolated and studied. They can be used as precursors to synthesize other aggregates if necessary.

Structures

The conductivity measurement of complex **2** suggests it to be a non-electrolyte in CH_2Cl_2. The ^{31}P-{^1H} NMR spectrum points to the chemical equivalence of all four phosphines (δ 19.7). Single-crystal X-ray diffraction analysis of **2** shows a symmetric chelation of the dithio ligand on the Hg^{II} with two similar Hg–S lengths [Hg(3)–S(2), 2.619(2) *vs.* Hg(3)–S(1), 2.641(3) Å]. This is the second crystallographically analysed addition complex of **1** with a binary transition metal chloride; the first such example is $[(Ph_3P)_4Pt_2(\mu_3\text{-}S)_2CoCl_2]$.[6] It shows the possibility for syn-

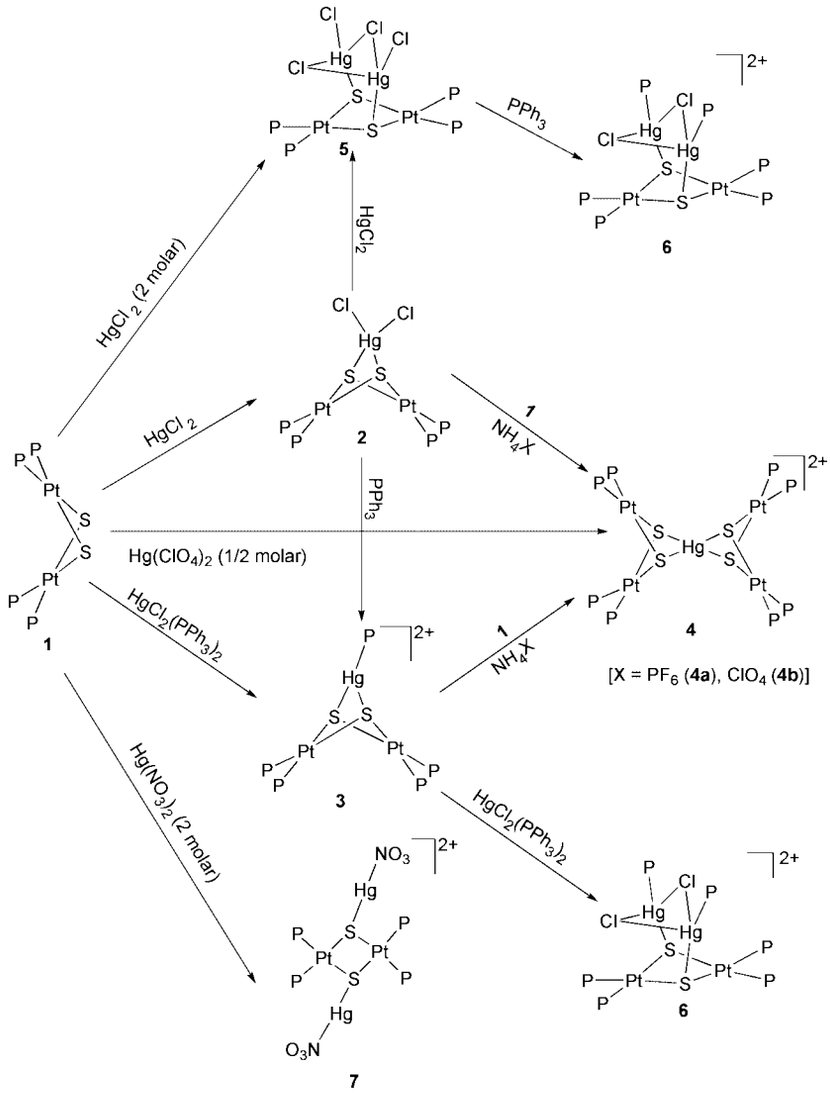

Scheme 1 Preparations and interconversions of complexes **2**–**7**.

thesizing a large range of Pt-containing sulfide aggregates in different heterometallic systems starting from basic materials such as MCl_n. Without formal Pt · · · Hg interactions (av. 3.301 Å), **2** is best treated as an aggregate, not a cluster, with a $\{HgPt_2S_2\}$ trigonal bipyramidal molecular core (Table 2 and Fig. 1). The local mercury(II) geometry is distorted tetrahedral with the ligand angles ranging from 120.39(11) [Cl(1)–Hg(3)–S(2)] to 71.86(7)° [S(2)–Hg(3)–S(1)]. The Hg–Cl distances [2.481(4) and 2.487(4) Å] are shorter than those found in $[HgCl_2(PPh_3)_2]$ [2.559(2) and 2.545(3) Å],[7] but comparable to the strong Hg–Cl bonds *e.g.* in $[HgCl_2\{Ph_2P(S)CH_2CH_2(S)PPh_2\}]$ [2.447(3) and 2.442(3) Å],[8] whilst the Hg–S bonds appear to be weak. The Hg–S distances are longer than the sum of covalent radii of Hg and S (2.52 Å).[9] This is consistent with the nature of the S→Hg bonds in this addition complex.

The conductivity measurement of complex **3b** suggests it to be a 2:1 electrolyte in acetone. X-Ray analysis of **3b** shows that the dithio ligand is asymmetrically co-ordinated to the Hg with a short and presumably strong Hg–S bond [2.428(2) Å] accompanied by a long, presumably weak Hg–S bond [2.694(2) Å] (Table 2 and Fig. 2). Coupled with two considerably different P–Hg–S angles [166.96(9), 116.65(8)°], the local geometry of Hg^{II} is best described as a distorted planar T shape in which $\{Pt_2S_2\}$ serves more as a semi-unidentate ligand. The Hg^{II} is merely 0.0886 Å above the least-squares plane. Although three-co-ordinated Hg^{2+} in T-shaped geometry is known, examples are rare.[10] This geometry is also rare among the vast collection

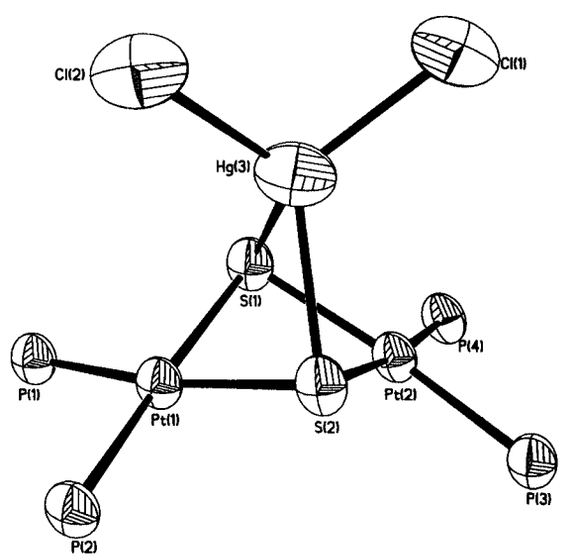

Fig. 1 Thermal ellipsoid plot (50% probability) of $[(Ph_3P)_4Pt_2(\mu_3\text{-}S)_2\text{-}HgCl_2]$ (phenyl rings are omitted for clarity).

of mixed-metal aggregates formed from **1**. The Hg(3)–P(5) distance [2.402(3) Å] is comparable to normal Hg–P bonds, *e.g.* $HgBr_2[R_2(R'O)P]$ [2.399(2) Å] (R_2P = bis(phosphonio)isophosphinodolide, R′ = Me).[11] Other bond features are comparable to those of the other heterometallic complexes obtained from **1**.

Table 1 Crystal data and structure refinement for $[(Ph_3P)_4Pt_2(\mu_3\text{-}S)_2HgCl_2]\cdot CH_2Cl_2$, **2**, $[(Ph_3P)Pt_2(\mu_3\text{-}S)_2Hg(PPh_3)][PF_6]_2\cdot H_2O$, **3b**, $[HgPt_4(PPh_3)_8(\mu_3\text{-}S)_4][ClO_4]_2\cdot 3.5CH_2Cl_2\cdot CH_3OH\cdot H_2O$, **4b**, $[(Ph_3P)_4Pt_2(\mu_3\text{-}S)_2Hg_2(\mu\text{-}Cl)_2Cl_2]\cdot CH_2Cl_2$, **5**, and $[(PH_3P)_4Pt_2(\mu_3\text{-}S)_2Hg_2(\mu\text{-}Cl)_2(PPh_3)_2][PF_6]_2\cdot CH_2Cl_2$ **6**

	2	**3b**	**4b**	**5**	**6**
Chemical formula	$C_{73}H_{62}Cl_4HgP_4Pt_2S_2$	$C_{90}H_{77}F_{12}HgOP_7Pt_2S_2$	$C_{148.5}H_{133}Cl_9HgO_{10}P_8Pt_4S_4$	$C_{73}H_{62}Cl_6Hg_2P_4Pt_2S_2$	$C_{109}H_{92}Cl_4F_{12}Hg_2P_8Pt_2S_2$
Formula weight	1859.80	2274.20	3753.55	2131.30	2874.87
T/K	293(2)	293(2)	293(2)	293(2)	293(2)
Crystal system	Triclinic	Monoclinic	Monoclinic	Monoclinic	Triclinic
Space group	$P\bar{1}$	$P2_1/n$	$C2/c$	$P2_1/c$	$P\bar{1}$
a/Å	16.4366(10)	18.1038(3)	37.0244(5)	14.769(4)	14.5458
b/Å	17.6321(3)	27.8444(1)	19.6785(3)	25.453(9)	17.4269
c/Å	18.2643(3)	20.9295(3)	28.0765(5)	23.201(9)	24.8814
α/°	114.730(10)	—	—	—	79.242(1)
β/°	102.828(10)	92.466(1)	127.432(1)	94.262(17)	88.898(1)
γ/°	98.010(10)	—	—	—	72.579(1)
V/Å^3	4523.73(11)	10540.6(2)	16243.7(4)	8698(5)	5907.55(14)
Z	2	4	4	4	2
μ/mm^{-1}	5.044	4.306	4.704	1.779	5.247
No. of reflections collected	25360	56758	48725	24902	51337
No. of unique data (R_{int})	17359 (0.0265)	21005 (0.0403)	17893 (0.0512)	17200 (0.1392)	25578 (0.0335)
$R1$/$wR2$ (obs. data)	0.0546, 0.1695	0.0520, 0.1534	0.0531, 0.1387	0.1045, 0.2377	0.0475, 0.1373
(all data)	0.0792, 0.1894	0.0837, 0.1707	0.0980, 0.1623	0.3091, 0.3266	0.0817, 0.1576

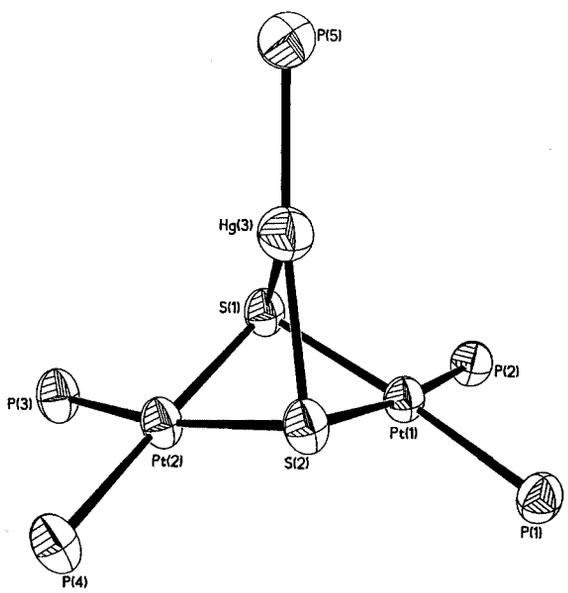

Fig. 2 Thermal ellipsoid plot of $[(Ph_3P)_4Pt_2(\mu_3\text{-}S)_2Hg(PPh_3)]^{2+}$ **3b**. Details as in Fig. 1.

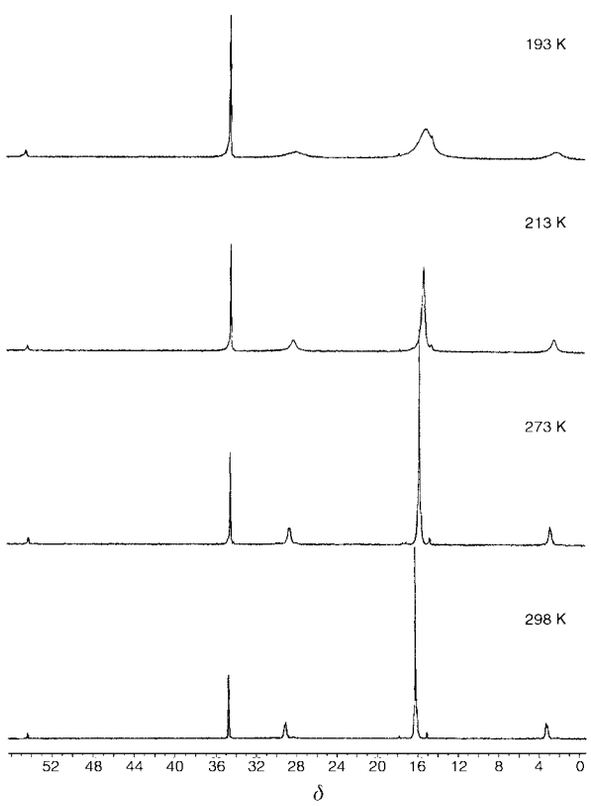

Fig. 3 V.T. $^{31}P\{^1H\}$ NMR of $[(Ph_3P)Pt_2(\mu_3\text{-}S)_2Hg(PPh_3)][PF_6]_2$ **3b** in CD_2Cl_2.

The $^{31}P\text{–}\{^1H\}$ NMR spectrum of complex **3b** shows a single Pt–phosphine signal at δ 16.2 [^1J(P–Pt) = 3160 Hz] and Hg-phosphine peak at δ 34.8 [^1J(P–Hg) = 4872 Hz]. It suggests that all the phosphines on the two Pt are equivalent, which violates the asymmetric disposition of the $[Hg(PPh_3)]$ moiety as found in the crystal structure. V.T. $^{31}P\text{-}\{^1H\}$ NMR analysis reveals that peak broadening begins at 213 K and the static state is not reached even at 193 K (Fig. 3). This points to a facile fluxional mechanism, which is likely described by a rapid flipping of the $[Hg(PPh_3)]$ moiety between the two sulfur centers. A similar fluxional process was also observed in our recently reported compound $[Pt_2S_2Au(PPh_3)_5][PF_6]$, which involves a trigonal planar transition state.[12]

The conductivity measurement of complex **4b** suggests it to be 2:1 electrolyte in CH_2Cl_2. X-Ray analysis of **4b** shows a distorted tetrahedral mercury(II) cationic complex stabilized by two $\{Pt_2S_2\}$ butterflies (Table 2 and Fig. 4). This complex was first described by Mingos and co-workers but its crystal structure has not been reported.[13] It is an unusual example of a "mononuclear" metal stabilized exclusively by ligand **1**, and the first crystallographically characterized example. A similar example of Cu^I, *viz*. $[Cu\{Pt_2(PPh_3)_4(\mu\text{-}S)_2\}_2][PF_6]_2$, was reported with spectroscopic evidence.[14] It has to be pointed out that a similar structure has been reported in the related pentametallic complexes $[M\{Pt_2(dppe)_2(\mu\text{-}S)_2\}_2]X_2$ (M = Zn, Cd or Hg).[15] The four Hg–S bond lengths (av. 2.620 Å) are close to those in **2** (av. 2.630 Å), implying that addition of another $\{Pt_2S_2\}$ core does not significantly affect the stability of the system.

The dihedral angle between the two S–Hg–S planes (120.1°) is significantly distorted from the ideal 90°. A similar phenomenon has been observed in $[M\{Pt_2(dppe)_2(\mu\text{-}S)_2\}_2]X_2$ (M = Zn, Cd or Hg).[15] It would suggest that in the static state the eight phosphine groups in **4b** would not be equivalent. The $^{31}P\text{-}\{^1H\}$ NMR analysis confirms this projection by showing two broad peaks at δ 18.5 [^1J(P–Pt) = 3290] and 14.4 [^1J(P–Pt) = 2960 Hz].

Table 2 Selected bond lengths (Å) and bond angles (°) for complexes **2**, **3b**, **4b**, **5** and **6**

$[(Ph_3P)_4Pt_2(\mu_3\text{-}S)_2HgCl_2]\cdot CH_2Cl_2$, **2**

Pt(1)–P(2)	2.283(2)	Pt(1)–P(1)	2.299(2)	Hg(3)–Cl(1)	2.481(4)	Hg(3)–Cl(2)	2.487(4)
Pt(1)–S(2)	2.345(2)	Pt(1)–S(1)	2.380(2)	Hg(3)–S(2)	2.619(2)	Hg(3)–S(1)	2.641(3)
Pt(2)–P(3)	2.298(2)	Pt(2)–P(4)	2.279(2)	Pt(1)···Hg(3)	3.296(7)	Pt(2)···Hg(3)	3.307(7)
Pt(2)–S(2)	2.382(2)	Pt(2)–S(1)	2.342(2)	Pt(1)···Pt(2)	3.254(7)	S(1)···S(2)	3.085(7)
P(2)–Pt(1)–P(1)	99.61(8)	P(2)–Pt(1)–S(2)	92.58(8)	Cl(2)–Hg(3)–S(2)	118.81(10)	Cl(1)–Hg(3)–S(1)	118.09(10)
S(2)–Pt(1)–S(1)	81.55(8)	S(1)–Pt(2)–S(2)	81.56(8)	Cl(2)–Hg(3)–S(1)	118.67(11)	S(2)–Hg(3)–S(1)	71.86(7)
Cl(1)–Hg(3)–Cl(2)	106.44(14)	Cl(1)–Hg(3)–S(2)	120.39(11)				

$[(Ph_3P)_4Pt_2(\mu_3\text{-}S)_2Hg(PPh_3)][PF_6]_2\cdot H_2O$, **3b**

Pt(1)–P(2)	2.300(2)	Pt(1)–P(1)	2.328(2)	Hg(3)–S(1)	2.694(2)	Hg(3)–S(2)	2.428(2)
Pt(1)–S(1)	2.360(2)	Pt(1)–S(2)	2.423(2)	Hg(3)–P(5)	2.402(3)	Pt(1)···Hg(3)	3.199(5)
Pt(2)–P(4)	2.308(2)	Pt(2)–P(3)	2.306(2)	Pt(2)···Hg(3)	3.189(5)	Pt(1)···Pt(2)	3.306(5)
Pt(2)–S(2)	2.386(2)	Pt(2)–S(1)	2.386(2)	S(1)···S(2)	3.144(5)		
P(2)–Pt(1)–P(1)	98.08(9)	P(2)–Pt(1)—S(1)	91.60(8)	P(5)–Hg(3)–S(1)	116.65(8)	S(2)–Hg(3)–S(1)	75.54(7)
P(1)–Pt(1)–S(1)	170.28(9)	P(2)–Pt(1)–S(2)	173.31(9)	Pt(1)–S(1)–Pt(2)	88.33(8)	Pt(1)–S(1)–Hg(3)	78.25(6)
P(1)–Pt(1)–S(2)	88.09(8)	S(1)–Pt(1)–S(2)	82.20(8)	Pt(2)–S(1)–Hg(3)	77.50(6)	Pt(2)–S(2)–Pt(1)	86.87(7)
S(1)–Pt(2)–S(2)	82.44(7)	P(5)–Hg(3)–S(2)	166.96(9)	Pt(2)–S(2)–Hg(3)	82.95(7)	Pt(1)–S(2)–Hg(3)	82.52(7)

$[HgPt_4(PPh_3)_8(\mu_3\text{-}S)_4][ClO_4]_2\cdot 3.5CH_2Cl_2\cdot CH_3OH\cdot H_2O$, **4b**

Pt(1)–P(2)	2.291(2)	Pt(1)–P(1)	2.312(2)	Hg(3)–S(1A)	2.628(2)	Hg(3)–S(1)	2.628(2)
Pt(1)–S(1A)	2.360(2)	Pt(1)–S(1)	2.374(2)	S(1)–Pt(1A)	2.360(2)	S(2)–Pt(2A)	2.375(2)
Pt(2)–P(3)	2.308(2)	Pt(2)–P(4)	2.287(2)	Hg···Pt(av.)	3.278	Pt···Pt(av.)	3.307
Pt(2)–S(2A)	2.375(2)	Pt(2)–S(2)	2.356(2)	S···S(av.)	3.073		
Hg(3)–S(2)	2.612(2)	Hg(3)–S(2A)	2.612(2)				
P(2)–Pt(1)–P(1)	96.68(9)	P(2)–Pt(1)–S(1A)	93.35(9)	S(2)–Hg(3)–S(2A)	71.88(10)	S(2)–Hg(3)–S(1A)	146.38(7)
P(1)–Pt(1)–S(1A)	169.94(9)	P(2)–Pt(1)–S(1)	172.09(9)	S(2A)–Hg(3)–S(1A)	118.64(7)	S(2)–Hg(3)–S(1)	118.64(7)
P(1)–Pt(1)–S(1)	88.90(8)	S(1A)–Pt(1)–S(1)	81.19(9)	S(2A)–Hg(3)–S(1)	146.38(7)	S(1A)–Hg(3)–S(1)	71.76(10)
P(4)–Pt(2)–P(3)	97.10(9)	P(4)–Pt(2)–S(2)	94.08(8)	Pt(1A)–S(1)–Pt(1)	89.10(8)	Pt(1A)–S(1)–Hg(3)	81.74(7)
P(3)–Pt(2)–S(2)	168.80(8)	P(4)–Pt(2)–S(2A)	174.22(8)	Pt(1)–S(1)–Hg(3)	81.47(7)	Pt(2)–S(2)–Pt(2A)	88.24(7)
P(3)–Pt(2)–S(2A)	88.01(8)	S(2)–Pt(2)–S(2A)	80.79(9)	Pt(2)–S(2)–Hg(3)	82.70(7)	Pt(2A)–S(2)–Hg(3)	82.33(7)

$[(Ph_3P)_4Pt_2\ (\mu_3\text{-}S)_2Hg_2(\mu\text{-}Cl)_2Cl_2]\cdot CH_2Cl_2$, **5**

Pt(2)–P(3)	2.269(9)	Pt(2)–P(4)	2.290(9)	Hg(1)–Cl(3)	2.365(9)	Hg(1)–S(1)	2.417(7)
Pt(2)–S(2)	2.366(8)	Pt(2)–S(1)	2.376(9)	Hg(1)–Cl(1)	2.777(10)	Hg(1)–Cl(2)	2.779(10)
Pt(1)–P(1)	2.301(9)	Pt(1)–P(2)	2.309(9)	Hg(1)–Pt(1)	3.834(9)	Hg(2)···Pt(1)	3.810(9)
Pt(1)–S(1)	2.352(8)	Pt(1)–S(2)	2.376(8)	Hg(1)···Pt(2)	3.752(9)	Hg(2)···Pt(2)	3.792(9)
Hg(2)–Cl(4)	2.365(10)	Hg(2)–S(2)	2.400(7)	Pt(1)···Pt(2)	2.398(9)	S(1)···S(2)	3.162(9)
Hg(2)–Cl(2)	2.710(9)	Hg(2)–Cl(1)	2.823(10)				
P(3)–Pt(2)–P(4)	100.7(3)	P(3)–Pt(2)–S(2)	89.9(3)	S(2)–Hg(2)–Cl(1)	104.3(3)	Cl(2)–Hg(2)–Cl(1)	86.6(3)
P(4)–Pt(2)–S(2)	166.3(3)	P(3)–Pt(2)–S(1)	173.5(3)	Cl(3)–Hg(1)–S(1)	144.4(4)	Cl(3)–Hg(1)–Cl(1)	101.4(4)
P(4)–Pt(2)–S(1)	85.5(3)	S(2)–Pt(2)–S(1)	83.6(3)	S(1)–Hg(1)–Cl(1)	103.5(3)	Cl(3)–Hg(1)–Cl(2)	102.1(4)
P(1)–Pt(1)–P(2)	101.2(3)	P(1)–Pt(1)–S(1)	90.1(3)	S(1)–Hg(1)–Cl(2)	104.6(3)	Cl(1)–Hg(1)–Cl(2)	86.2(3)
P(2)–Pt(1)–S(1)	167.0(3)	P(1)–Pt(1)–S(2)	173.9(3)	Pt(1)–S(1)–Pt(2)	91.9(3)	Pt(1)–S(1)–Hg(1)	107.0(3)
P(2)–Pt(1)–S(2)	84.6(3)	S(1)–Pt(1)–S(2)	84.0(3)	Pt(2)–S(1)–Hg(1)	103.0(3)	Hg(1)–Cl(1)–Hg(2)	81.5(3)
Cl(4)–Hg(2)–S(2)	145.2(3)	Cl(4)–Hg(2)–Cl(2)	99.9(3)	Pt(2)–S(2)–Pt(1)	91.6(3)	Pt(2)–S(2)–Hg(2)	105.4(3)
S(2)–Hg(2)–Cl(2)	103.5(3)	Cl(4)–Hg(2)–Cl(1)	102.4(4)	Pt(1)–S(2)–Hg(2)	105.8(3)	Hg(2)–Cl(2)–Hg(1)	83.5(2)

$[(Ph_3P)_4Pt_2(\mu_3\text{-}S)_2Hg_2(\mu\text{-}Cl)_2(PPh_3)_2][PF_6]_2\cdot CH_2Cl_2$, **6**

Pt(1)–P(1)	2.292(2)	Pt(1)–P(2)	2.304(2)	Hg(2)–S(2)	2.396(2)	Hg(2)–P(6)	2.434(2)
Pt(1)–S(1)	2.361(2)	Pt(1)–S(2)	2.377(2)	Hg(2)–Cl(1)	2.775(2)	Hg(2)–Cl(2)	2.781(2)
Pt(2)–P(3)	2.300(2)	Pt(2)–P(4)	2.321(2)	Hg(1)···Hg(2)	3.529(2)	Pt(1)···Pt(2)	3.382(2)
Pt(2)–S(2)	2.366(2)	Pt(2)–S(1)	2.383(2)	S(1)···S(2)	3.136(2)	Pt(1)···Hg(1)	3.722(2)
Hg(1)–P(5)	2.450(2)	Hg(1)–S(1)	2.453(2)	Pt(1)···Hg(2)	3.906(2)	Pt(2)···Hg(1)	3.948(2)
Hg(1)–Cl(1)	2.616(2)	Hg(1)–Cl(2)	2.679(2)	Pt(2)···Hg(2)	3.785(2)		
P(1)–Pt(1)–P(2)	97.21(8)	P(1)–Pt(1)–S(1)	92.94(7)	S(1)–Hg(1)–Cl(2)	102.82(8)	Cl(1)–Hg(1)–Cl(2)	89.02(7)
P(2)–Pt(1)–S(1)	168.66(7)	P(1)–Pt(1)–S(2)	175.66(7)	S(2)–Hg(2)–P(6)	158.16(8)	S(2)–Hg(2)–Cl(1)	102.94(7)
P(2)–Pt(1)–S(2)	86.85(7)	S(1)–Pt(1)–S(2)	82.88(7)	P(6)–Hg(2)–Cl(1)	95.26(8)	S(2)–Hg(2)–Cl(2)	106.75(7)
P(3)–Pt(2)–P(4)	97.79(9)	P(3)–Pt(2)–S(2)	90.97(8)	P(6)–Hg(2)–Cl(2)	86.94(8)	Cl(1)–Hg(2)–Cl(2)	83.85(7)
P(4)–Pt(2)–S(2)	168.50(8)	P(3)–Pt(2)–S(1)	173.56(8)	Pt(1)–S(1)–Pt(2)	90.95(7)	Pt(1)–S(1)–Hg(1)	101.25(8)
P(4)–Pt(2)–S(1)	88.41(8)	S(2)–Pt(2)–S(1)	82.65(7)	P(2)–S(1)–Hg(1)	109.42(8)	Pt(2)–S(2)–Pt(1)	91.00(7)
P(5)–Hg(1)–S(1)	131.60(8)	P(5)–Hg(1)–Cl(1)	106.98(8)	Pt(2)–S(2)–Hg(2)	105.28(8)	Pt(1)–S(2)–Hg(2)	109.87(8)
S(1)–Hg(1)–Cl(1)	110.60(7)	P(5)–Hg(1)–Cl(2)	107.25(8)	Hg(1)–Cl(1)–Hg(2)	81.72(7)	Hg(1)–Cl(2)–Hg(2)	80.52(6)

It is interesting that a similar phenomenon is not observed in $[Cu\{Pt_2(PPh_3)_4(\mu\text{-}S)_2\}_2][PF_6]_2$[14] or $[M\{Pt_2(dppe)_2(\mu\text{-}S)_2\}_2]X_2$ (M = Zn, Cd or Hg).[15]

The $^{31}P\text{-}\{^1H\}$ NMR of complex **5** shows the phosphine at δ 21.6 [^1J(P–Pt) = 2999 Hz]. The chlorides are non-dissociating, as reflected in its non-electrolytic behavior in CH_2Cl_2. The crystal structure shows an unusual Hg_2 cation stabilized by bridging **1** and two bridging chlorides. With another terminal chloride on each Hg^{II}, this completes a tetrahedral geometry for the metal (Table 2 and Fig. 5). This provides the first crystallographic evidence of the $\{Pt_2M_2S_2\}$ system in which $\{Pt_2S_2\}$ remains hinged. Comparison of **2**, **3**, **4** and **5** illustrates that

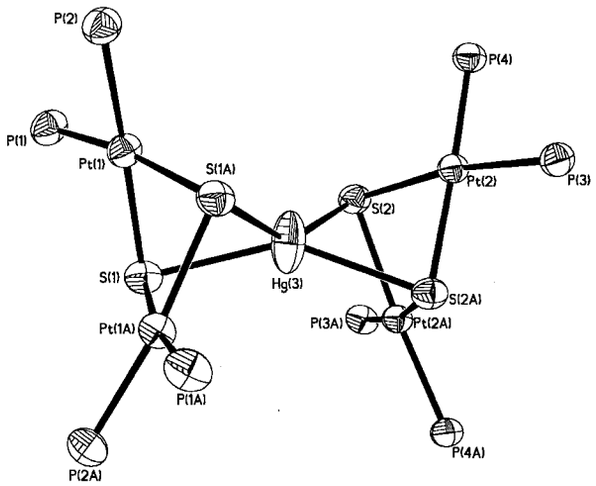

Fig. 4 Thermal ellipsoid plot of $[HgPt_4(PPh_3)_8(\mu_3\text{-}S)_4]^{2+}$. Details as in Fig. 1.

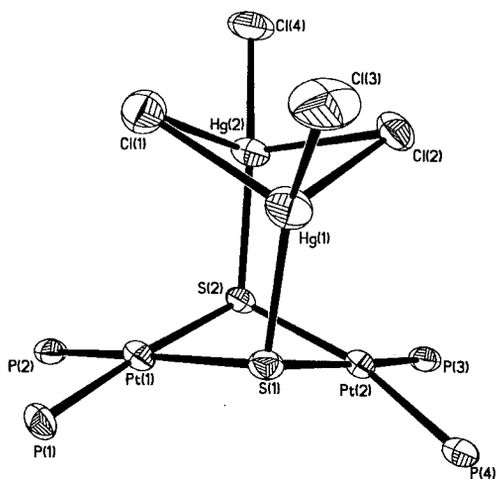

Fig. 5 Thermal ellipsoid plot of $[(Ph_3P)_4Pt_2(\mu_3\text{-}S)_2Hg_2(\mu\text{-}Cl)_2Cl_2]$ **5**. Details as in Fig. 1.

structurally these systems are complex and adaptive and that the final product in these syntheses is often a delicate balance of substrate stoichiometry, choice of ligands and reaction conditions. Not surprisingly, the bridging Hg–Cl bonds [av. 2.772(8) Å] are significantly longer than the terminal Hg–Cl bonds [av. 2.365(8) Å] in **5** and Hg–Cl bond length [av. 2.484(4) Å] in **2**. Accordingly, the two Hg–S bonds [av. 2.409(7) Å] are significantly stronger than those of **2**. This reflects the different bonding nature, and perhaps chemical reactivities, of these similar complexes. It also offers optimism that further aggregation can occur (based on **5**) without losing the Hg–S bonds.

The $^{31}P\text{-}\{^1H\}$ NMR spectrum of complex **6** gives one Pt–phosphine peak at δ 19.9 [^1J(P–Pt) = 3066 Hz] and another peak for the Hg–phosphine at δ 34.9 [^1J(P–Hg) = 5490 Hz]. The conductivity measurement of **6** suggests it to be a 2:1 electrolyte in acetone. The crystal structure shows a Hg_2 core supported by a bridging dithio, two bridging chlorides and two terminal phosphines, which is analogous to that of **5** (Table 2 and Fig. 6). The displacement of chloride by a good σ donor, PPh_3, does not change the structure significantly. Both **5** and **6** can be viewed as a fusion of two butterflies, *viz*. $\{Pt_2S_2\}$ and $\{Hg_2Cl_2\}$ across the Hg–S bonds.

Addition of $Hg(NO_3)_2$ to complex **1** (1:2) gives $[(Ph_3P)_4Pt_2(\mu_3\text{-}S)_2Hg_2(NO_3)_2][NO_3]_2$ **7a**, which can be metathesized to give $[(Ph_3P)_4Pt_2(\mu_3\text{-}S)_2Hg_2(NO_3)_2][PF_6]_2$ **7b**. Although attempts to grow single crystals of **7a** or **7b** suitable for X-ray study have been unsuccessful, their identities can be deduced from their spectroscopic, conductivity and elemental analysis data

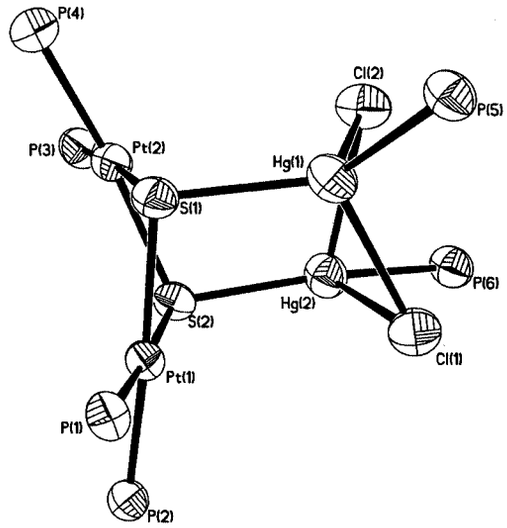

Fig. 6 Thermal ellipsoid plot of $[(Ph_3P)_4Pt_2(\mu_3\text{-}S)_2Hg_2(\mu\text{-}Cl)_2(PPh_3)_2]^{2+}$ **6**. Details as in Fig. 1.

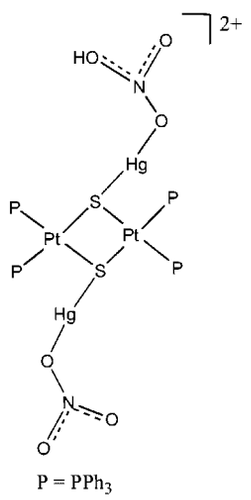

Fig. 7 Proposed structure for $[(Ph_3P)_4Pt_2(\mu_3\text{-}S)_2Hg_2(NO_3)_2]^{2+}$ **7** (phenyl rings are omitted for clarity).

(Fig. 7). The IR spectrum of **7b** shows peaks at 1382 and 841 cm^{-1} that correspond to co-ordinated NO_3^- and unco-ordinated PF_6^-. The $^{31}P\text{-}\{^1H\}$ NMR of **7b** shows one peak at δ 18.7 [^1J(P–Pt) = 3033 Hz]. Its structure is likely to be similar to that of $[(Ph_3P)_4Pt_2(\mu_3\text{-}S)_2M_2Cl_2]$ (M = Au[2] or Ag[3]) whereby two MCl "molecular pendants" are anchored on the flat Pt_2S_2.

Some important bond lengths of complexes **2**, **3b**, **4b, 5** and **6** are compared in Table 3. Although **1** can support the heterometal Hg in different geometries to give different addition products, the $\{Pt_2S_2\}$ ring parameters remain fairly constant in terms of its Pt–S bonds, S···S and Pt···Pt distances.

Electrochemistry

Cyclic voltammetry (CV) studies of complexes **2**, **3b**, **5** and **6** were carried out to investigate their redox behavior. The CV of **3b** (Fig. 8(a)) shows an approximately reversible one-electron transfer oxidation with $E_{p,a}$ = 1.10 V and $E_{p,c}$ = 1.01 V (ΔE = 90 mV). The $i_{p,c}$:$i_{p,a}$ ratio was about 0.7, indicating some decay of the product of the initial oxidation. This peak has not been assigned at this stage. A similar redox peak was also observed for the complexes $[(Ph_3P)_4Pt_2(\mu\text{-}S)_2HgFc][PF_6]_2$ (Fc = $(C_5H_5)_2Fe$)[16] and $[(Ph_3P)_4Pt_2(\mu\text{-}S)_2Au(PPh_3)]Cl$.[17] The possible redox couples in this compound are Pt^{II}–Pt^{III}, Hg^{II}–Hg^{III} and S^{-II}–S^{-I}. We examined the electrochemical behaviors of a series $Pt_2(PPh_3)_4(\mu\text{-}S)_2$ complexes. $Pt^{II}Pt^{III}$ did not show electro-

Table 3 Comparison of important bond lengths (Å) of complexes **2**, **3b**, **4b**, **5** and **6**

	2	**3b**	**4b**	**5**	**6**
Pt–S	2.345(2)	2.360(2)	2.360(2)	2.352(8)	2.361(2)
	2.380(2)	2.423(2)	2.374(2)	2.376(8)	2.377(2)
	2.382(2)	2.386(2)	2.375(2)	2.376(9)	2.366(2)
	2.342(2)	2.386(2)	2.356(2)	2.366(8)	2.383(2)
Hg–S	2.641(3)	2.694(2)	2.612(2)	2.400(7)	2.453(2)
	2.619(2)	2.428(2)	2.628(2)	2.417(7)	2.396(2)
Hg–Cl(terminal)	2.484(4) (av.)			2.365(9) (av.)	
Hg–Cl(bridge)				2.772(8) (av.)	2.713(2) (av.)
					2.450(2)
Hg–P		2.402(3)			2.434(2)
av. Hg · · · Pt	3.301	3.194	3.278	3.797	3.840
Pt · · · Pt	3.254	3.306	3.307 (av.)	3.398	3.382
S · · · S	3.085	3.144	3.073 (av.)	3.162	3.136
Pt–S–S–Pt/°	132.7	135.5	131	143.3	138.8

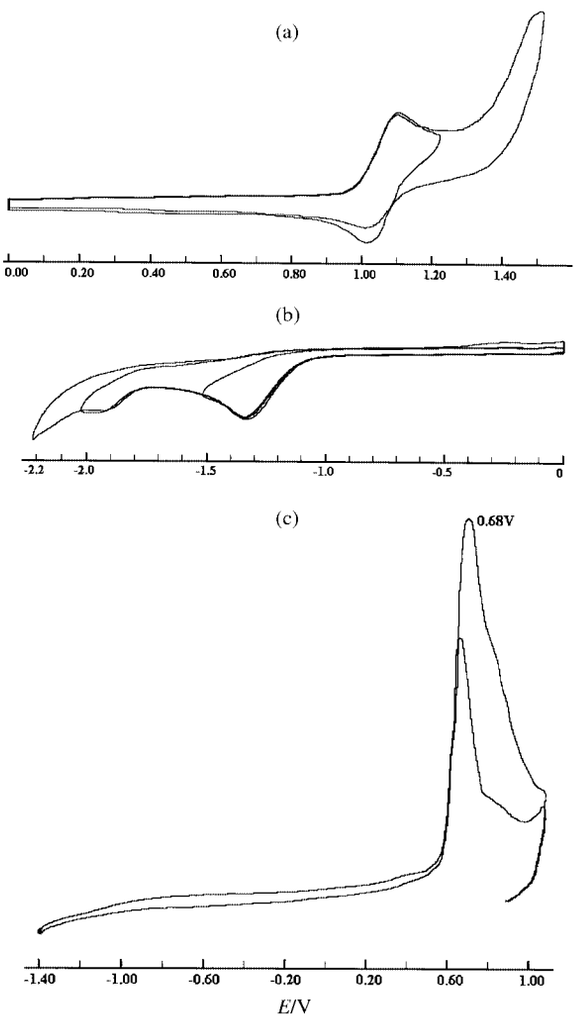

Fig. 8 Cyclic voltammetric scans of complex $[(Ph_3P)_4Pt_2(\mu_3\text{-}S)_2\text{-}Hg(PPh_3)][PF_6]_2 \cdot H_2O$ **3b**: (a) anodic scans from 0.00 to 1.50 V (scan rate 50 mV/s^{-1}), (b) cathodic scans from −0.00 to −2.20 V (scan rate 100 mV/s^{-1}) and (c) scanning from −1.40 to 1.10 V holding at −1.40 V for (1) 0 s and (2) 10 s (scan rate 100 mV/s^{-1}).

chemical activity under similar experimental conditions. Although Hg^{III} can be generated electrochemically with a hard ligand such as 1,4,8,11-tetraazacyclotetradecane ([14]aneN$_4$) at a very low temperature,[18] it is unlikely that Hg^{III} can be stabilized by our thio-based metalloligand. The S^{-II}–S^{-I} redox couple is also unlikely to show reversible properties. Our tentative inference is that this peak is related to an oxidation process of a delocalized electron in the HOMO in the molecule. Further investigation of this redox couple is in progress. The reduction of this complex shows two irreversible waves before the background breaks down, with peak potentials at −1.34 and −1.93 V. The first wave was also found for one of the other complexes studied here (**6**). This peak was assigned to the reduction of Hg^{II} to Hg^0. This assignment is supported by the observation that when the potential was held at −1.60 V, for a period of time, followed by an anodic scan, a sharp oxidation peak at E_p = 0.68 V (Fig. 8(b)) was observed. This sharp peak is attributed to the stripping of the Hg^0 formed on the electronic surface at −1.60 V. Further, the peak height increased with time held at −1.60 V (Fig. 8(c)). For the other two complexes (**2** and **5**) this first reduction wave is absent. This is possibly explained by the electron donating affect of PPh_3, which supports the reduction of complexes **3b** and **6** better compared to that of **2** and **5**. The second reduction wave (Fig. 8(b)) was present for all the four complexes studied. This reduction process has not been assigned.

Table 4 Cyclic voltammetric data of complexes **2**, **3b**, **5** and **6**

		Cathodic scan	
Compound	Anodic scan E_p/V	$E_{p,Hg(II)/Hg(0)}$/V	E_p/V
2	0.94	—	−2.03
3b	$E_{p,a}$ = 1.10	−1.34	−1.93
	$E_{p,c}$ = 1.01		
5	0.93	—	−2.01
6	1.05	−1.53	−2.05

All waves were irreversible except for the oxidation of compound **3b**.

The CV of the oxidation of complex **6** showed two irreversible waves; the first (≈ 1.05 V) is smaller than the second (≈ 1.30 V). Both are poorly defined with the second almost merging with the background breakdown.

Both complexes **2** and **5** show a broad, irreversible oxidation wave at 0.94 V. This wave appears to be due to a multiple process. (The CVs of complexes **2**, **5** and **6** are not shown here.) The electrochemical data for all the complexes are summarized in Table 4.

Conclusion

The successful assembly of different metallic systems described in this paper is attributed to the ability of the $\{Pt_2S_2\}$ chromophore to function as a semi-unidentate, chelating and bridging ligand. This behavior, when coupled with the flexible geometric modes of the heterometal(s), allows us to assemble a range of aggregates of increasing nuclearities. The sequential nature of network assembly also points to the possibility of introducing different metals at different stages, thus marking a positive step towards our target of electroactive multimetallic assembly. This is a topic in our future discussions.

Acknowledgements

The authors acknowledge the National University of Singapore (NUS) for financial support. Z. Li thanks NUS for a research scholarship award. X. Xu thanks NUS for a postdoctoral fellowship. Technical support from the Department of Chemistry of NUS is appreciated.

References

1 S. W. A. Fong and T. S. A. Hor, *J. Chem. Soc.*, *Dalton Trans.*, 1999, 639.
2 W. Bos, J. I. Bour, P. P. J. Schlebos, P. Hageman, W. P. Bosman, J. M. M. Smits, J. A. C. van Wietmarschen and P. T. Beurskens, *Inorg. Chim. Acta*, 1986, **119**, 141.
3 H. Liu, A. L. Tan, C. R. Cheng, K. F. Mok and T. S. A. Hor, *Inorg. Chem.*, 1997, **36**, 2916.
4 R. Ugo, G. La Monica, S. Cenimi, A. Segre and F. Conti, *J. Chem. Soc. A*, 1971, 522.
5 G. M. Sheldrick, SHELXL 93, Program for Crystal Structure Refinement, University of Göttingen, 1993.
6 H. Liu, A. L. Tan, K. F. Mok and T. S. A. Hor, *J. Chem. Soc.*, *Dalton Trans.*, 1996, 4023.
7 N. A. Bell, T. D. Dee, M. Goldstein, P. J. McKenna and I. W. Nowell, *Inorg. Chim. Acta*, 1983, **71**, 135.
8 T. S. Lobana, M. K. Sandhu, M. J. Liddell and E. R. T. Tiekink, *J. Chem. Soc.*, *Dalton Trans.*, 1990, 691.
9 D. Grdenic, *Q. Rev. Chem. Soc.*, 1965, **19**, 303.
10 A. J. Canty and B. M. Gatehouse, *J. Chem. Soc.*, *Dalton Trans.*, 1976, 2018.
11 D. Gudat, M. Nieger and M. Schrott, *Inorg. Chem.*, 1997, **36**, 1476.
12 Z. Li, Z.-H. Loh, K. F. Mok and T. S. A. Hor, *Inorg. Chem.*, submitted for publication.
13 E. Briant, T. S. A. Hor, N. D. Howells and D. M. P. Mingos, *J. Chem. Soc.*, *Chem. Commun.*, 1983, 1118.
14 H. Liu, A. L. Tan, Y. Xu, K. F. Mok and T. S. A. Hor, *Polyhedron*, 1997, **16**, 377.
15 M. Capdevila, Y. Carrasco, W. Clegg, R. A. Coxall, P. González-Duate, A. Lledós and J. A. Ramírez, *J. Chem. Soc.*, *Dalton Trans.*, 1999, 3103.
16 S.-W. Audi Fong, X. Xu, J. J. Vittal, W. Henderson, S. B. Khoo and T. S. Andy Hor, *Angew. Chem.*, *Int. Ed.*, submitted for publication.
17 Z. Li, K. F. Mok, S. B. Khoo and T. S. Andy Hor, unpublished work, 2000.
18 R. L. Deming, A. L. Allred, A. R. Dahl, A. W. Herlinger and M. O. Kestner, *J. Am. Chem. Soc.*, 1976, **98**, 4132.
19 G. M. Sheldrick, SADABS, Program for Siemens area detector absorption correction, University of Göttingen, Germany, 1996.